

Contribution from the Department of Chemistry and Biochemistry, University of Arkansas, Fayetteville, Arkansas 72701, AT&T Bell Laboratories, Murray Hill, New Jersey 07974, and Guelph Waterloo Centre for Graduate Work in Chemistry, Guelph Campus, Department of Chemistry and Biochemistry, University of Guelph, Guelph, Ontario N1G 2W1, Canada

Preparation and Solid-State Structures of (Cyanophenyl)dithia- and (Cyanophenyl)diselenadiazolyl Radicals

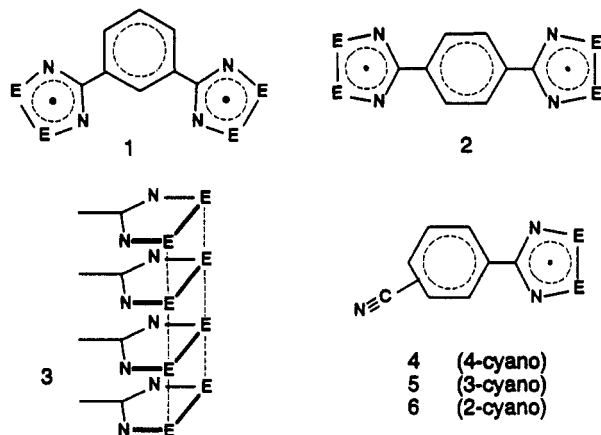
A. W. Cordes,^{1a} R. C. Haddon,^{1b} R. G. Hicks,^{1c} R. T. Oakley,^{*,1c} and T. T. M. Palstra^{1b}

Received August 8, 1991

The preparation and solid-state characterization of the dimers of the cyanophenyl-substituted 1,2,3,5-dithia- and 1,2,3,5-diselenadiazolyl radicals $[\text{NCC}_6\text{H}_4\text{CN}_2\text{E}_2]^{\bullet}$ ($\text{E} = \text{S}, \text{Se}$) are described. Crystals of the 4-cyanophenyl derivatives **4** are triclinic, space group $P\bar{1}$. The radicals dimerize in a cofacial fashion, with mean intradimer E...E spacings of 3.104/3.233 Å ($\text{E} = \text{S}/\text{Se}$). The dimer units form ribbonlike arrays connected by head-to-tail CN...E contacts. The ribbons are packed in an antiparallel fashion with no close interdimer E...E contacts. The 3-cyanophenyl sulfur derivative **5** crystallizes in two phases. The α -phase, along with the isomorphous selenium compound, belongs to the monoclinic space group $P2_1/n$. As in the 4-cyano derivatives, the radicals dimerize cofacially, generating ribbons connected by head-to-tail CN...E contacts. The ribbons, however, are layered with CN_2E_2 rings oriented into stacks parallel to the a axis. In addition to short intradimer E...E contacts (mean values = 3.13 (2)/3.27 (4) Å for $\text{E} = \text{S}/\text{Se}$), there are relatively short interdimer E...E contacts (mean values = 4.26 (5)/4.15 (5) Å ($\text{E} = \text{S}/\text{Se}$)) along the stacking axis. The β -phase of the 3-cyanophenyl sulfur compound **5**, monoclinic space group $P2_1/n$, forms discrete dimers associated in a trans antarafacial fashion, with intradimer S...S contacts of 3.121 (1) Å; there are no close interdimer S...S contacts. The 2-cyanophenyl selenium derivative **6** crystallizes in the polar space group $P2_1$. In this structure also the dimer units are laced together by short CN...Se contacts. The dimers form stacks parallel to the b axis, with mean intradimer and interdimer Se...Se contacts of 3.312/4.083 Å, respectively. Lattice constants for the six structures are: **4** ($\text{E} = \text{S}$), $\text{C}_8\text{H}_4\text{N}_2\text{S}_2$, $a = 10.466$ (3) Å, $b = 10.342$ (2) Å, $c = 9.169$ (2) Å, $\alpha = 104.97$ (2)°, $\beta = 112.97$ (2)°, $\gamma = 69.84$ (2)°, $V = 849.0$ (3) Å³, $Z = 4$; **4** ($\text{E} = \text{Se}$), $\text{C}_8\text{H}_4\text{N}_2\text{Se}_2$, $a = 10.478$ (4) Å, $b = 10.780$ (4) Å, $c = 9.432$ (4) Å, $\alpha = 107.16$ (3)°, $\beta = 115.23$ (2)°, $\gamma = 68.39$ (3)°, $V = 883.8$ (6) Å³, $Z = 4$; **5** ($\text{E} = \text{S}$, α -phase), $\text{C}_8\text{H}_4\text{N}_2\text{S}_2$, $a = 7.295$ (3) Å, $b = 20.488$ (2) Å, $c = 11.276$ (2) Å, $\beta = 95.54$ (2)°, $V = 1676.0$ (7) Å³, $Z = 8$; **5** ($\text{E} = \text{Se}$), $\text{C}_8\text{H}_4\text{N}_2\text{Se}_2$, $a = 7.364$ (8) Å, $b = 21.085$ (2) Å, $c = 11.119$ (4) Å, $\beta = 94.91$ (5)°, $V = 1720$ (7) Å³, $Z = 8$; **5** ($\text{E} = \text{S}$, β -phase), $\text{C}_8\text{H}_4\text{N}_2\text{S}_2$, $a = 8.782$ (1) Å, $b = 5.638$ (1) Å, $c = 17.128$ (4) Å, $\beta = 102.94$ (2)°, $V = 826.5$ (6) Å³, $Z = 4$; **6** ($\text{E} = \text{Se}$), $\text{C}_8\text{H}_4\text{N}_2\text{Se}_2$, $a = 7.301$ (1) Å, $b = 11.883$ (2) Å, $c = 10.186$ (1) Å, $\beta = 101.50$ (1)°, $V = 866.1$ (5) Å³, $Z = 4$.

Introduction

We recently reported the preparation and structural and electronic characterization of 1,3- and 1,4-phenylene-bridged 1,2,3,5-dithiadiazolyl and 1,2,3,5-diselenadiazolyl biradicals $[(\text{E}_2\text{N}_2\text{C})\text{C}_6\text{H}_4(\text{CN}_2\text{E}_2)]^{1,2,3}$ and **2**⁴ ($\text{E} = \text{S}, \text{Se}$). This work has



evolved from our interest⁵ in the design of molecular conductors based on the use of neutral rather than charged radicals as molecular building blocks. All these bifunctional radicals associate in the solid state, but the packing pattern for dimers, and even the mode of association, vary considerably. The dimers of the 1,4 derivatives ($\text{E} = \text{S}, \text{Se}$) adopt a herring-bone-like packing pattern, while the 1,3 derivatives ($\text{E} = \text{S}, \text{Se}$) stack in vertical

arrays, with association occurring in a zigzag fashion through opposite ends of the diradical. The selenium-based 1,3-phenylene system also crystallizes in a second (or β -) phase, in which the crescentlike dimers generate chainlike arrays. All the structures, particularly the selenium derivatives, are characterized by short intradimer E...E contacts. Single-crystal conductivity studies suggest that both phases of the selenium-based 1,3 derivatives are intrinsic semiconductors, with band gaps of 0.55 and 0.77 eV for the α - and β -phases, respectively.

In order to understand better the molecular features that influence solid-state architecture, we have turned our attention to the packing patterns of "custom-built" monofunctional radicals. To date, the structural evidence on simple dithiadiazolyl dimers $[\text{RCN}_2\text{S}_2]_2$ ($\text{R} = \text{Ph}, \text{Me}, \text{NMe}_2, \text{CF}_3$)⁶ provides no indication that the desired⁵ mode of packing, i.e., vertical arrays of cofacially aligned "plates", as in **3**, can be obtained. The structure of $[\text{PhCN}_2\text{Se}_2]_2$, the only characterized selenium-based monofunctional radical dimer, is more encouraging, showing weak Se...Se interactions between the dimer units.⁷ In an attempt to influence the solid-state packing of dimer units in a controllable way, we have synthesized and structurally characterized the 2-, 3-, and 4-cyanophenyl-substituted radicals **4**, **5** ($\text{E} = \text{S}, \text{Se}$), and **6** ($\text{E} = \text{Se}$). The idea behind this strategy can be traced back to the structure of *p*-iodobenzonitrile and, indeed, to that of the cyanogen halides XCN ($\text{X} = \text{Cl}, \text{Br}, \text{I}$).⁸ In the solid state all of these systems adopt a packing pattern in which the molecules align themselves into ribbonlike chains, with close CN...X contacts (i.e. weak $\text{N}(\text{lone pair})/\text{X}-\text{C}(\sigma^*)$ interactions) acting as molecular

- (1) (a) University of Arkansas. (b) AT&T Bell Laboratories. (c) University of Guelph.
- (2) Andrews, M. P.; Cordes, A. W.; Douglass, D. C.; Fleming, R. M.; Glarum, S. H.; Haddon, R. C.; Marsh, P.; Oakley, R. T.; Palstra, T. T. M.; Schneemeyer, L. F.; Trucks, G. W.; Tycko, R.; Waszczak, J. V.; Young, K. M.; Zimmerman, N. M. *J. Am. Chem. Soc.* **1991**, *113*, 3559.
- (3) Cordes, A. W.; Haddon, R. C.; Hicks, R. G.; Oakley, R. T.; Palstra, T. T. M.; Schneemeyer, L. N.; Waszczak, J. V.; Zimmerman, N. M. *J. Am. Chem. Soc.* **1992**, *114*, 1729.
- (4) Cordes, A. W.; Haddon, R. C.; Oakley, R. T.; Schneemeyer, L. F.; Waszczak, J. V.; Young, K. M.; Zimmerman, N. M. *J. Am. Chem. Soc.* **1991**, *113*, 582.

- (5) (a) Haddon, R. C. *Nature (London)* **1975**, *256*, 394. (b) Haddon, R. C. *Aust. J. Chem.* **1975**, *28*, 2343.
- (6) (a) Vegas, A.; Pérez-Salazar, A.; Banister, A. J.; Hey, R. G. *J. Chem. Soc., Dalton Trans.* **1980**, 1812. (b) Hofs, H.-U.; Bats, J. W.; Gleiter, R.; Hartmann, G.; Mews, R.; Eckert-Maksić, M.; Oberhammer, H.; Sheldrick, G. M. *Chem. Ber.* **1985**, *118*, 3781. (c) Banister, A. J.; Hansford, M. I.; Hauptmann, Z. V.; Wait, S. T.; Clegg, W. *J. Chem. Soc., Dalton Trans.* **1989**, 1705. (d) Cordes, A. W.; Goddard, J. D.; Oakley, R. T.; Westwood, N. P. C. *J. Am. Chem. Soc.* **1989**, *111*, 6147.
- (7) Del Bel Belluz, P.; Cordes, A. W.; Kristof, E. M.; Kristof, P. V.; Liblong, S. W.; Oakley, R. T. *J. Am. Chem. Soc.* **1989**, *111*, 9276.
- (8) (a) Schlemper, E. O.; Britton, D. *Acta Crystallogr.* **1965**, *18*, 419. (b) Heiart, R. B.; Carpenter, G. B. *Acta Crystallogr.* **1965**, *9*, 889 and references cited therein.

Table I. Atomic Coordinates for Non-Hydrogen Atoms of the Dimer of **4** (E = S)^a

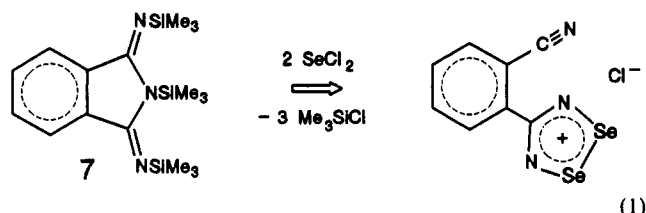
	x	y	z	B _{iso} ^b Å ²
S1	0.28535 (8)	-0.01677 (8)	0.24784 (9)	2.58 (2)
S2	0.45107 (8)	0.01456 (9)	0.2017 (1)	2.73 (2)
S3	0.05577 (8)	0.16456 (9)	-0.0075 (1)	2.50 (2)
S4	0.21970 (8)	0.19921 (8)	-0.0546 (1)	2.58 (2)
N1	0.2792 (3)	-0.1597 (3)	0.1212 (3)	2.56 (7)
N2	0.4641 (3)	-0.1228 (3)	0.0666 (3)	2.60 (7)
N3	0.0408 (3)	0.0297 (3)	-0.1468 (3)	2.38 (7)
N4	0.2237 (3)	0.0703 (3)	-0.2013 (3)	2.53 (7)
N5	0.3832 (5)	-0.7719 (4)	-0.5242 (5)	6.3 (1)
N6	0.1155 (5)	-0.5611 (4)	-0.8167 (5)	6.4 (1)
C1	0.3727 (4)	-0.1957 (3)	0.0422 (3)	2.21 (8)
C2	0.3766 (4)	-0.3237 (3)	-0.0763 (3)	2.15 (8)
C3	0.4596 (4)	-0.3548 (4)	-0.1745 (4)	2.78 (8)
C4	0.4635 (4)	-0.4714 (4)	-0.2857 (4)	3.11 (9)
C5	0.3841 (4)	-0.5602 (4)	-0.3022 (4)	2.99 (9)
C6	0.3021 (4)	-0.5310 (3)	-0.2045 (4)	3.08 (9)
C7	0.2983 (4)	-0.4132 (3)	-0.0929 (3)	2.78 (9)
C8	0.3847 (5)	-0.6808 (4)	-0.4245 (5)	4.3 (1)
C9	0.1288 (4)	-0.0005 (3)	-0.2311 (3)	2.20 (8)
C10	0.1204 (4)	-0.1179 (3)	-0.3633 (3)	2.13 (8)
C11	0.1990 (4)	-0.1436 (4)	-0.4658 (4)	2.73 (8)
C12	0.1928 (4)	-0.2542 (4)	-0.5873 (4)	3.27 (9)
C13	0.1099 (4)	-0.3416 (4)	-0.6071 (4)	3.06 (9)
C14	0.0308 (4)	-0.3139 (4)	-0.5061 (4)	3.3 (1)
C15	0.0353 (4)	-0.2031 (4)	-0.3864 (4)	2.84 (8)
C16	0.1110 (5)	-0.4631 (4)	-0.7270 (5)	4.1 (1)

^a ESDs refer to the last digit printed. ^b B_{iso} is the mean of the principal axes of the thermal ellipsoid.

ties. In the present paper we report the preparation and solid-state structures of the radical dimers of **4**, **5** (E = S, Se), and **6** (E = Se).

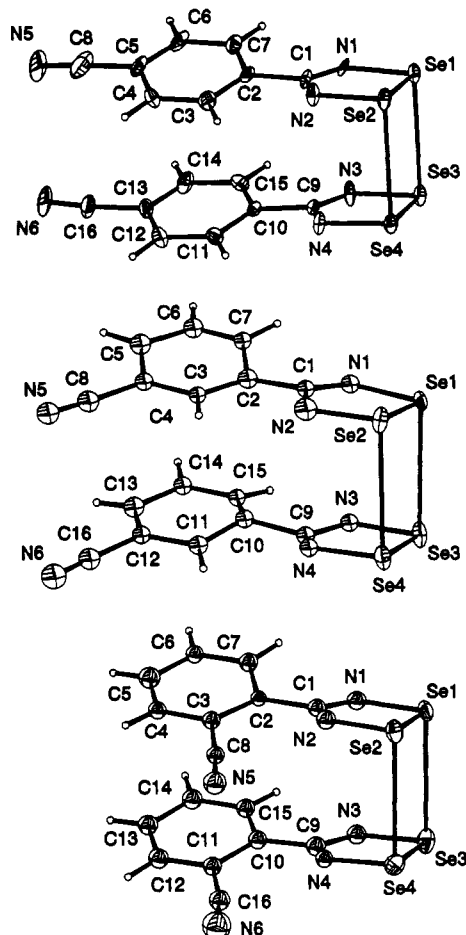
Results

Preparation of Radicals and Radical Dimers. The 3- and 4-cyanophenyl-substituted dithia- and diselenadiazolium cations necessary for the production of **4** and **5** were prepared by condensation of either the free cyanobenzamidine or its *N,N*-bis(trimethylsilyl) lithium salt with sulfur or selenium dichloride. The 2-cyanophenyl-substituted diselenadiazolium cation was prepared by the condensation of the bicyclic derivative **7** with selenium dichloride (eq 1). We have been unable to prepare the



corresponding dithiadiazolium cation in good yield from this reagent. The radicals were generated directly from the parent cations by reduction with triphenylantimony and purified by vacuum sublimation at 120–160 °C/10⁻² Torr, which afforded the radical dimers. In the case of the dimer of the 3-cyanophenyl sulfur radical **5** (E = S), two crystalline phases, hereafter termed α (needles) and β (blocks) could be grown. This behavior is reminiscent of the polymorphism exhibited by the biradical **1** (E = Se). A second phase of the dimer of the 2-cyanophenyl selenium radical **6** (E = Se) was also obtained, in addition to the blocklike crystals characterized below, but the feathery nature of this phase rendered it unsuitable for structural analysis.

Crystal Structures. The six crystal structures reported here can be divided into two groups. The larger group consists of radical dimers [NCC₆H₄(CN₂E₂)₂]₂ exhibiting a cofacial geometry, i.e., **4** (E = S, Se), **5** (E = Se, S (α -phase)) and **6** (E = Se). ORTEP drawings of dimers of **4–6** (E = Se), illustrating the atom numbering schemes and characteristic twisting of the phenyl rings with respect to the CN₂E₂ ring, are provided in Figure 1. Tables I–VI list atomic coordinates, while Table VII summarizes the intradimer E–E and interdimer E...E distances (other internal structural

**Figure 1.** ORTEP drawings of radical dimers of **4–6** (E = Se), showing atom numbering. Atom numbering of **4** and **5** (E = S) is equivalent.**Table II.** Atomic Coordinates for Non-Hydrogen Atoms of the Dimer of **4** (E = Se)^a

	x	y	z	B _{iso} ^b Å ²
Se1	0.2717 (2)	-0.0055 (2)	0.2601 (2)	2.26 (8)
Se2	0.4732 (2)	0.0121 (2)	0.2319 (2)	2.31 (7)
Se3	0.0436 (2)	0.1756 (2)	-0.0066 (2)	2.29 (8)
Se4	0.2394 (2)	0.1991 (2)	-0.0407 (2)	2.25 (8)
N1	0.271 (1)	-0.158 (1)	0.114 (1)	1.9 (5)
N2	0.478 (1)	-0.138 (1)	0.084 (1)	2.3 (6)
N3	0.037 (1)	0.030 (1)	-0.160 (1)	2.8 (6)
N4	0.237 (1)	0.054 (1)	-0.198 (1)	2.4 (6)
N5	0.375 (2)	-0.758 (2)	-0.516 (2)	7 (1)
N6	0.122 (2)	-0.557 (2)	-0.811 (2)	8 (1)
C1	0.372 (2)	-0.196 (1)	0.052 (2)	2.0 (7)
C2	0.373 (2)	-0.322 (1)	-0.070 (2)	2.0 (7)
C3	0.443 (2)	-0.347 (2)	-0.172 (2)	2.9 (8)
C4	0.445 (2)	-0.462 (2)	-0.288 (2)	3.4 (8)
C5	0.376 (2)	-0.554 (1)	-0.295 (2)	3.0 (7)
C6	0.304 (2)	-0.526 (1)	-0.193 (2)	3.1 (8)
C7	0.304 (2)	-0.410 (1)	-0.078 (2)	2.4 (7)
C8	0.378 (2)	-0.671 (2)	-0.418 (2)	6 (1)
C9	0.132 (1)	-0.004 (1)	-0.226 (2)	1.8 (7)
C10	0.125 (2)	-0.121 (1)	-0.361 (2)	1.6 (6)
C11	0.192 (2)	-0.142 (1)	-0.466 (2)	2.4 (7)
C12	0.191 (2)	-0.251 (2)	-0.589 (2)	2.8 (8)
C13	0.115 (2)	-0.341 (1)	-0.602 (2)	3.2 (8)
C14	0.044 (2)	-0.319 (2)	-0.502 (2)	3.2 (8)
C15	0.0480 (2)	-0.208 (2)	-0.3800 (2)	2.5 (8)
C16	0.115 (2)	-0.462 (2)	-0.727 (2)	4 (1)

^a ESDs refer to the last digit printed. ^b B_{iso} is the mean of the principal axes of the thermal ellipsoid.

parameters are available in the supplementary material).

In all cases the internal E–E bonds and the intradimer E...E separations are reminiscent of those seen in both the monofunctional and bifunctional radical dimers reported previously. In

Table III. Atomic Coordinates for Non-Hydrogen Atoms of the Dimer of **5** (E = S, α -Phase)^a

	x	y	z	$B_{iso}, \text{\AA}^2$
S1	0.7746 (3)	0.02372 (8)	0.2038 (2)	3.81 (8)
S2	0.8070 (3)	-0.03688 (9)	0.3523 (2)	3.85 (9)
S3	1.1841 (3)	0.00208 (8)	0.1596 (2)	3.70 (8)
S4	1.2275 (3)	-0.05129 (8)	0.3170 (2)	3.72 (8)
N1	0.7014 (8)	-0.0338 (3)	0.1131 (5)	3.8 (3)
N2	0.7434 (8)	-0.1035 (2)	0.2787 (5)	3.5 (3)
N3	1.1281 (8)	-0.0606 (2)	0.0768 (5)	3.3 (3)
N4	1.1809 (8)	-0.1216 (2)	0.2523 (5)	3.5 (3)
N5	0.634 (1)	-0.3816 (3)	0.1039 (7)	5.3 (4)
N6	1.162 (1)	-0.4057 (3)	0.1476 (7)	5.8 (4)
C1	0.6938 (8)	-0.0926 (3)	0.1638 (6)	2.8 (3)
C2	0.6220 (8)	-0.1467 (3)	0.0845 (5)	2.7 (3)
C3	0.6478 (8)	-0.2114 (3)	0.1208 (6)	2.7 (3)
C4	0.5851 (8)	-0.2609 (3)	0.0439 (6)	2.9 (3)
C5	0.4965 (9)	-0.2476 (3)	-0.0691 (6)	3.1 (3)
C6	0.4719 (9)	-0.1831 (3)	-0.1026 (6)	3.4 (3)
C7	0.5361 (9)	-0.1336 (3)	-0.0273 (6)	3.0 (3)
C8	0.614 (1)	-0.3282 (4)	0.0788 (6)	3.5 (3)
C9	1.1343 (8)	-0.1173 (3)	0.1354 (6)	2.6 (3)
C10	1.0892 (8)	-0.1773 (3)	0.0660 (6)	2.8 (3)
C11	1.1225 (8)	-0.2379 (3)	0.1185 (6)	2.8 (3)
C12	1.0858 (8)	-0.2942 (3)	0.0511 (6)	2.8 (3)
C13	1.014 (1)	-0.2903 (3)	-0.0663 (7)	3.5 (3)
C14	0.9804 (9)	-0.2297 (3)	-0.1175 (6)	3.4 (3)
C15	1.0188 (8)	-0.1740 (3)	-0.0518 (6)	3.4 (3)
C16	1.127 (1)	-0.3572 (4)	0.1055 (7)	4.0 (4)

^a ESDs refer to the last digit printed. ^b B_{iso} is the mean of the principal axes of the thermal ellipsoid.

Table IV. Atomic Coordinates for Non-Hydrogen Atoms of the Dimer of **5** (E = Se)^a

	x	y	z	$B_{iso}, \text{\AA}^2$
Se1	0.7859 (6)	0.0252 (2)	0.1868 (4)	2.7 (2)
Se2	0.7962 (6)	-0.0356 (2)	0.3606 (4)	3.2 (2)
Se3	1.2168 (6)	0.0054 (2)	0.1620 (4)	3.1 (2)
Se4	1.2391 (6)	-0.0524 (2)	0.3402 (4)	3.1 (2)
N1	0.711 (4)	-0.041 (1)	0.092 (2)	2.4 (6)*
N2	0.737 (4)	-0.108 (1)	0.272 (3)	3.7 (7)*
N3	1.156 (4)	-0.062 (1)	0.077 (2)	2.2 (6)*
N4	1.182 (4)	-0.125 (1)	0.263 (3)	2.3 (6)*
N5	0.640 (4)	-0.377 (2)	0.113 (3)	3.5 (7)*
N6	1.160 (5)	-0.398 (2)	0.138 (3)	4.4 (9)*
C1	0.690 (5)	-0.096 (2)	0.166 (3)	2.1 (8)*
C2	0.641 (5)	-0.151 (2)	0.081 (3)	2.7 (8)*
C3	0.660 (5)	-0.212 (2)	0.123 (3)	2.0 (7)*
C4	0.601 (5)	-0.262 (2)	0.049 (3)	2.3 (8)*
C5	0.499 (6)	-0.251 (2)	-0.066 (4)	3 (1)*
C6	0.480 (5)	-0.188 (2)	-0.100 (3)	2.8 (8)*
C7	0.535 (4)	-0.142 (2)	-0.029 (3)	2.1 (7)*
C8	0.628 (6)	-0.329 (2)	0.086 (4)	3.2 (9)*
C9	1.163 (5)	-0.117 (2)	0.141 (3)	2.3 (8)*
C10	1.089 (5)	-0.175 (2)	0.067 (3)	2.3 (8)*
C11	1.141 (5)	-0.234 (2)	0.118 (3)	2.5 (8)*
C12	1.091 (5)	-0.288 (2)	0.042 (3)	2.3 (8)*
C13	1.017 (5)	-0.283 (2)	-0.071 (4)	2.9 (9)*
C14	0.982 (5)	-0.223 (2)	-0.116 (3)	2.3 (8)*
C15	1.037 (5)	-0.171 (2)	-0.050 (3)	2.0 (7)*
C16	1.130 (5)	-0.353 (2)	0.097 (3)	3.2 (9)*

^a ESDs refer to the last digit printed. ^b B_{iso} is the mean of the principal axes of the thermal ellipsoid. The starred atoms were refined isotropically.

contrast to these cofacial dimers, the dimeric unit in the β -phase of the 3-cyanophenyl sulfur derivative **5** (E = S) adopts a trans-antarafacial geometry (Figure 2), the two dimer halves being related by a crystallographic center of symmetry. Such an arrangement is reminiscent of the structures adopted by salts of the $[\text{S}_3\text{N}_2]_2^{2+}$ dication.⁹ The S---S separation of 3.141 (1) Å remains similar to those seen in the more common cofacial dimers. The

Table V. Atomic Coordinates for Non-Hydrogen Atoms of the Dimer of **5** (E = S, β -Phase)^a

	x	y	z	$B_{iso}, \text{\AA}^2$
S1	0.29623 (6)	0.4299 (1)	-0.05590 (3)	2.67 (1)
S2	0.35495 (6)	0.7422 (1)	0.00927 (3)	2.60 (1)
N1	0.1929 (2)	0.3220 (4)	0.0036 (1)	2.50 (4)
N2	0.2619 (2)	0.6706 (3)	0.0778 (1)	2.49 (4)
N5	-0.0155 (2)	0.7177 (4)	0.3633 (1)	3.68 (5)
C1	0.1922 (2)	0.4588 (4)	0.0671 (1)	2.21 (4)
C2	0.1078 (2)	0.3749 (4)	0.1277 (1)	2.21 (4)
C3	0.1023 (2)	0.5173 (4)	0.1936 (1)	2.31 (4)
C4	0.0169 (2)	0.4422 (4)	0.2480 (1)	2.42 (4)
C5	-0.0608 (3)	0.2260 (4)	0.2386 (1)	2.94 (4)
C6	-0.0528 (3)	0.0851 (4)	0.1740 (1)	3.03 (5)
C7	0.0308 (3)	0.1586 (4)	0.1188 (1)	2.67 (4)
C8	0.0020 (3)	0.5950 (4)	0.3136 (1)	2.69 (4)

^a ESDs refer to the last digit printed. ^b B_{iso} is the mean of the principal axes of the thermal ellipsoid.

Table VI. Atomic Coordinates for Non-Hydrogen Atoms of the Dimer of **6** (E = Se)^a

	x	y	z	$B_{iso}, \text{\AA}^2$
Se1	0.8154 (3)	1.16600	0.6046 (2)	3.1 (1)
Se2	0.8282 (3)	0.9883 (3)	0.5119 (2)	3.2 (1)
Se3	0.3577 (3)	1.1661 (3)	0.5467 (2)	3.5 (1)
Se4	0.3606 (3)	0.9878 (3)	0.4536 (2)	3.3 (1)
N1	0.831 (2)	1.112 (1)	0.767 (2)	2.7 (3)*
N2	0.850 (2)	0.932 (1)	0.672 (2)	2.8 (3)*
N3	0.359 (2)	1.1130 (1)	0.709 (2)	2.8 (3)*
N4	0.361 (2)	0.931 (1)	0.615 (1)	2.2 (3)*
N5	0.687 (2)	0.693 (2)	0.748 (2)	4.0 (4)*
N6	0.185 (3)	0.6970 (2)	0.684 (2)	6.2 (6)*
C1	0.844 (2)	0.999 (2)	0.773 (2)	2.4 (3)*
C2	0.861 (2)	0.951 (1)	0.909 (2)	1.8 (3)*
C3	0.814 (3)	0.840 (2)	0.934 (2)	2.4 (4)*
C4	0.833 (3)	0.799 (2)	1.064 (2)	2.4 (4)*
C5	0.898 (3)	0.869 (2)	1.172 (2)	3.4 (4)*
C6	0.952 (2)	0.974 (2)	1.149 (2)	2.4 (4)*
C7	0.940 (3)	1.016 (2)	1.0210 (2)	2.7 (4)*
C8	0.744 (3)	0.761 (2)	0.826 (2)	2.4 (4)*
C9	0.356 (3)	1.000 (2)	0.716 (2)	2.8 (4)*
C10	0.365 (3)	0.948 (2)	0.847 (2)	2.5 (4)*
C11	0.304 (3)	0.838 (2)	0.865 (2)	2.5 (4)*
C12	0.314 (3)	0.798 (2)	0.994 (2)	2.9 (4)*
C13	0.383 (3)	0.862 (2)	1.105 (2)	2.9 (4)*
C14	0.442 (3)	0.970 (2)	1.089 (2)	3.0 (4)*
C15	0.427 (3)	1.012 (2)	0.962 (2)	2.5 (4)*
C16	0.234 (3)	0.767 (2)	0.756 (2)	3.2 (4)*

^a ESDs refer to the last digit printed. ^b B_{iso} is the mean of the principal axes of the thermal ellipsoid. The starred atoms were refined isotropically.

Table VII. Intra- and Intermolecular Distances (Å) for Dimers of **4** (E = S, Se), **5** (E = S (α -phase), Se), and **6** (E = Se)

compd	4		5		6
E	S	Se	S	Se	Se
(E-E) ^a	2.081 (1)	2.317 (3)	2.080 (3)	2.318 (6)	2.325 (4)
(E---E) ^b	3.10 (2)	3.23 (4)	3.13 (2)	3.27 (4)	3.31 (3)
(E---E') ^c			4.26 (5)	4.15 (5)	4.08 (4)
d ₃ ^d	3.977 (1)	3.890 (3)	4.170 (3)	3.837 (3)	4.066 (4)
d ₄ ^d	3.926 (1)	3.829 (3)	4.168 (3)	3.930 (3)	4.040 (4)

^a Mean endocyclic E-E bond (range). ^b Mean intradimer E---E bond (range). ^c Mean interdimer E---E' contacts (range) along the stacking direction, i.e., mean of d₁ and d₂ in Figures 4 and 5. ^d Lateral interdimer E---E' contacts defined in Figures 3-5 and text.

crystal structure, however, affords no alignment of dimer units and, as a result, there are no notably close interdimer S---S contacts. Within the context of low-dimensional molecular conductors, the crystal structures of the cofacial dimers of **4-6** provide a useful insight into the importance of interactions within and between molecular stacks based on the CN_2E_2 building block. Details of the structural motifs adopted by the three systems are provided below.

(9) Gillespie, R. J.; Kent, J. P.; Sawyer, J. F. *Inorg. Chem.* **1981**, *20*, 3784 and references therein.

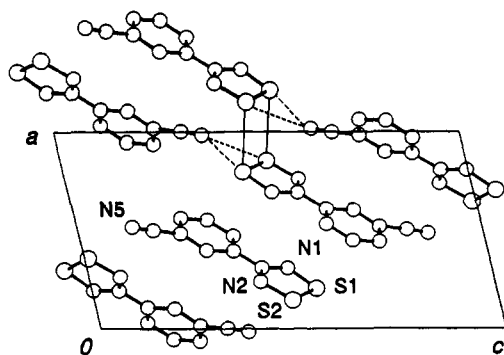


Figure 2. Unit cell drawing of radical dimer of β -phase of **5** ($E = S$), showing atom-numbering scheme and intradimer S...S linkages. Intermolecular CN...S contacts are shown by dashed lines.

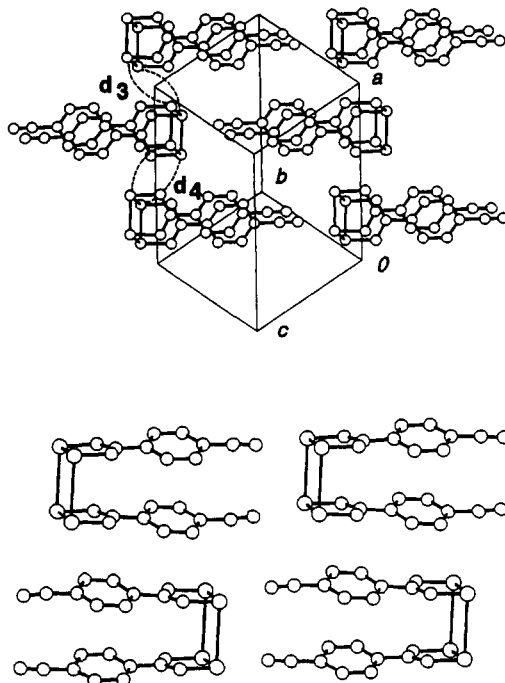


Figure 3. Unit cell drawing of **4** ($E = Se$) (above), showing ribbons of dimers connected by intermolecular CN...Se contacts; close lateral interdimer Se...Se' contacts d_3 and d_4 are indicated by dashed lines. Stacking of ribbons is shown below.

[4-NCC₆H₄(CN₂E₂)₂]₂. Crystals of the dimers of the 4-phenyl derivatives **4** ($E = S, Se$) are isomorphous and belong to the triclinic space group $P\bar{1}$. As anticipated, the crystal structure consists of ribbons of dimers packed in a head-to-tail fashion, with CN...E contacts (mean 3.04/3.11 Å for $E = S/Se$) linking consecutive molecules (Figure 3). Dimer units in adjacent ribbons are in relatively close proximity, as indicated by the E...E contacts d_3 ($E1...E3'$) and d_4 ($E2...E4'$) (mean of d_3 and $d_4 = 3.95$ (2)/3.86 (3) Å for $E = S/Se$). Ribbons stacked on top of one another, however, run in antiparallel directions. As a consequence, there is no alignment of the radical dimers between consecutive layers.

α -[3-NCC₆H₄(CN₂E₂)₂]₂. Crystals of this phase are monoclinic, space group $P2_1/n$. As in the 4-cyanophenyl derivatives the dimers are linked in a head-to-tail fashion by CN...E links (mean value 3.075/3.21 Å for $E = S/Se$), a feature which generates snakelike ribbons that weave across the yz plane in the y direction (Figure 4). As in the 4-cyanophenyl derivatives, there are close E...E contacts between adjacent ribbons in the same plane. These contacts, which span crystallographic inversion centers, arise from quite different molecular approaches, one being the head-on $E2...E4'$ contact d_3 (4.170 (3)/3.837 (3) Å for $E = S/Se$), the other the side-on $E1...E3'$ contact d_4 (4.168 (3)/3.930 (3) Å for $E = S/Se$). In addition to these interactions between ribbons, and in contrast to the packing found for the 4-cyanophenyl com-

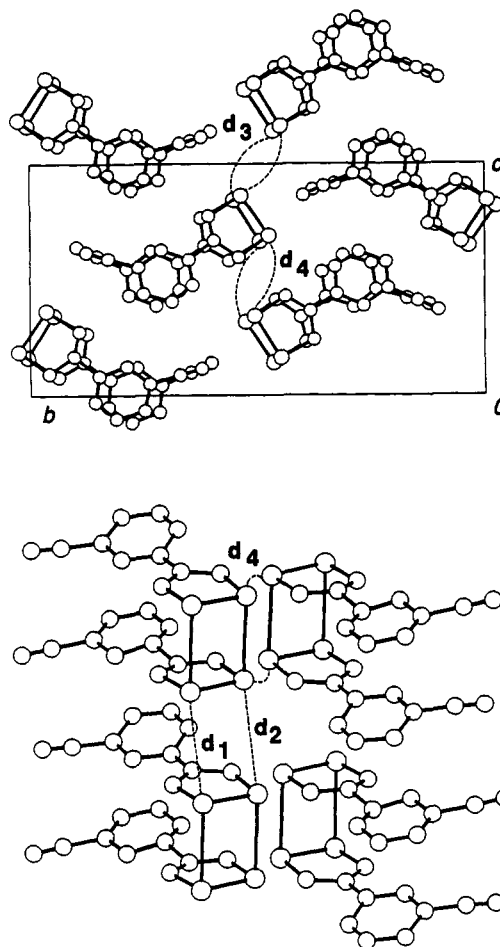


Figure 4. Unit cell drawing of **5** ($E = Se$) (above), showing network of dimers connected by intermolecular CN...Se contacts; close lateral interdimer Se...Se' contacts d_3 and d_4 are indicated by dashed lines. Stacking of dimers and definition of vertical interdimer Se...Se' contacts d_1 and d_2 are shown below.

pound described above, the stacking of dimer ribbons in the x direction produces a nearly vertical array of radical dimers, one only offset from perpendicularity by deviation ($5.54/4.91^\circ$ for $E = S/Se$) of the unit cell β -angle from 90° . Interdimer contacts d_1 and d_2 in the x direction for $E = S$ (mean 4.26 (5) Å) are well outside the van der Waals separation¹⁰ but for $E = Se$ (mean 4.15 (5) Å) are of structural significance. These contacts, for both $E = S$ and Se , when taken with the corresponding intradimer E...E contacts, produce a stacking pattern which is similar to, although less tight than, that observed in the structures of the α -phase of **1** ($E = S, Se$).

[2-NCC₆H₄(CN₂Se₂)₂]₂. Copper-colored blocks of **6** ($E = Se$) belong to the polar monoclinic space group $P2_1$; the crystal packing of the dimers is illustrated in Figure 5. The dimers lie in sheets in the yz plane and form extended arrays in the y direction linked by head-to-tail CN...Se contacts (mean 3.07 Å). As in both the 4- and 3-cyanophenyl derivatives there are close approaches between adjacent dimers; these interactions are characterized by the $Se2...Se3'$ and $Se1...Se4'$ contacts d_3 and d_4 (mean value = 4.05 (1) Å). As in the 3-cyanophenyl compounds the radical dimers stack along x in a nearly vertical fashion, although the offset from perpendicularity is now 11.5° . Relatively close interdimer Se...Se contacts (mean 4.083 Å) are, however, still maintained.

Summary and Conclusions

The cyanophenyl group serves as an effective structure-influencing ligand when attached to dithia- and diselenadiazolyl radicals. The CN...S/Se interactions which are produced in the

(10) Bondi, A. J. *Phys. Chem.* **1964**, *68*, 441.

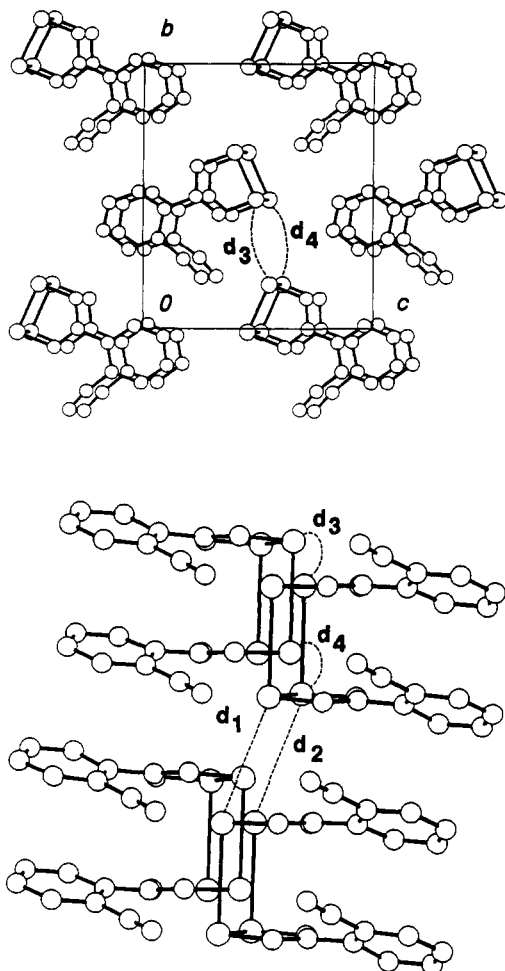


Figure 5. Unit cell drawing of **6** ($E = \text{Se}$), showing network of dimers connected by intermolecular $\text{CN} \cdots \text{Se}$ contacts (above). Close interdimer $\text{Se} \cdots \text{Se}$ contacts d_3 and d_4 are indicated by dashed lines. Stacking of dimers and definition of vertical interdimer $\text{Se} \cdots \text{Se}'$ contacts d_1 and d_2 are shown below.

solid-state link radical dimers into approximately coplanar ribbons. The resulting networks are characterized by $\text{E} \cdots \text{E}$ contacts to adjacent ribbons which, in general, are longer than the corresponding contacts in the structures of phenylene-bridged bifunctional radicals. However, it is interesting that here, as in the bifunctional systems, the interstack $\text{Se} \cdots \text{Se}$ contacts are closer than the corresponding $\text{S} \cdots \text{S}$ approaches. To the extent that orbital overlap can be considered to be operative, such interactions are binding the selenium-based materials together more effectively. Alignment of consecutive layers of ribbons so as to generate vertical or pseudovertically arrays of CN_2E_2 dimers, as found for the 2- and 3-cyano derivatives, is a hitherto unobserved feature for a monofunctional dithiadiazolyl or diselenadiazolyl radical. However, while the desired stacking mode is observed in the 2- and 3-cyano structures, the interdimer contacts d_1 and d_2 are longer than those seen in the α -phase of the 1,3-phenylene-bridged bifunctional radicals; the long $\text{E} \cdots \text{E}$ contacts in these latter compounds are 3.966 Å for $E = \text{S}$ and 4.014 Å for $E = \text{Se}$. The longer contacts (less compressed stacking) in the present systems may simply be a reflection of the deviation from purely vertical ordering.

As a result of the greater distortion away from a uniformly spaced array of radicals, i.e., **3**, the band gap in these materials is expected to be greater than in the previously described bifunctional materials, indeed the 4-cyano materials are insulators. Single-crystal conductivity measurements on the 3-cyano selenium compound **5** ($E = \text{Se}$), whose structural and thermal properties are the best of the present series, are shown in Figure 6. The room-temperature conductivity (ca. $10^{-9} \text{ S cm}^{-1}$) is over 4 orders of magnitude lower than that of the needle phase of the related

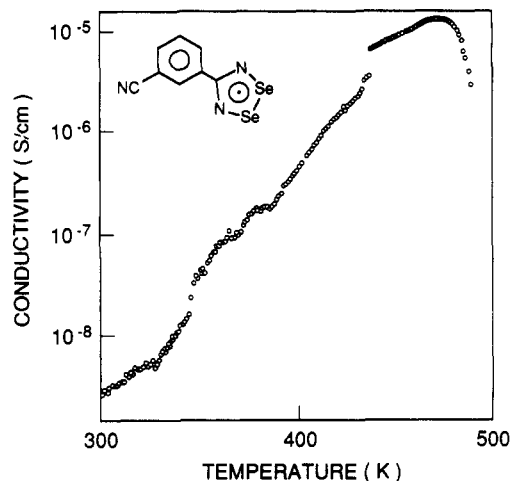


Figure 6. Single crystal conductivity of **5** ($E = \text{Se}$) as a function of temperature.

1,3-biradical **1**. In the context of optimizing packing patterns and close interradsical contacts, it is interesting to consider whether materials based on bifunctional radicals that incorporate cyano groups may lead to better conductivity characteristics than are observed in materials based only on one of these features.

Experimental Section

Starting Materials and General Procedures. 1,2-, 1,3- and 1,4-dicyanobenzene, lithium bis(trimethylsilyl)amide, trimethylsilyl chloride, sulfur dichloride, selenium powder, and triphenylantimony were all obtained commercially (Aldrich). Sulfur dichloride was distilled prior to use, and $\text{LiN}(\text{SiMe}_3)_2$ was converted to its diethyl etherate in order to facilitate amidine synthesis.¹¹ Compound **7** was prepared by a modification of the synthesis reported in the literature.¹² Accordingly, 1,2-dicyanobenzene and $\text{LiN}(\text{SiMe}_3)_2$ were reacted together in a 1:1 mole ratio (instead of 1:2) in toluene, and the mixture was then quenched with trimethylsilyl chloride. The product was distilled at 120 °C/0.1 Torr (yield 78%) to give an orange liquid which solidified on cooling to room temperature. The infrared spectrum of this material was in agreement with the literature data.¹² Acetonitrile (Fisher HPLC grade) was purified by distillation over P_2O_5 . All reactions were performed under an atmosphere of nitrogen. Selenium tetrachloride was prepared using the literature method.¹³ Mass spectra (70 eV, EI) were recorded on a Kratos MS890 mass spectrometer. Infrared spectra (CsI optics, Nujol mulls) were obtained on a Nicolet 20SX/C FTIR instrument. Elemental analyses were performed by MHW Laboratories, Phoenix, AZ.

Preparation of 4-Cyanobenzamidine.¹⁴ Solid $\text{LiN}(\text{SiMe}_3)_2 \cdot \text{Et}_2\text{O}$ (15.2 g, 63 mmol) was added to a slurry of 1,4-dicyanobenzene (11.3 g, 88 mmol) in 120 mL of diethyl ether, and the reaction was stirred for 2 h. The reaction mixture was then poured onto 200 mL of 0.1 M HCl, and after the two layers were filtered and separated, the aqueous solution was heated to 80 °C and filtered. The pale yellow mother filtrate was made basic with aqueous sodium hydroxide, and the white solid precipitate so obtained was filtered, air-dried, and recrystallized from an ethanol/toluene mixture (yield 4.4 g, 48%).

Preparation of 3-Cyanobenzamidine. Solid $\text{LiN}(\text{SiMe}_3)_2 \cdot \text{Et}_2\text{O}$ (24.2 g, 0.10 mol) was added to a slurry of 1,3-dicyanobenzene (11.8 g, 92 mmol) in 100 mL of ether. After 20 min all solid material had dissolved, giving a pale yellow solution which was poured onto 200 mL of 10% HCl. The aqueous layer was separated and made basic with aqueous sodium hydroxide. The heavy white precipitate was filtered off, washed with cold water, air-dried, and recrystallized from an ethanol/toluene solution (yield 9.7 g, 73%).

Preparation of *N*-Lithio-*N'*,*N'*-bis(trimethylsilyl)-*x*-cyanobenzamidine ($x = 3, 4$). These two compounds were prepared by a modification of the procedure used for the simple amidines (vide supra). In typical preparations toluene was added to an ethereal solution of the *N*-lithiated derivative obtained by the treatment of the nitrile with $\text{LiN}(\text{SiMe}_3)_2$.

- (11) Boeré, R. T.; Oakley, R. T.; Reed, R. W. *J. Organomet. Chem.* **1987**, 331, 161.
- (12) Weller, F.; Schmück, F.; Dehnicke, K. *Z. Naturforsch.* **1989**, 44B, 548.
- (13) Brauer, G. *Handbook of Preparative Chemistry*; Academic: New York, 1963; Vol. 1, p. 423.
- (14) This compound has also been made by a Sandmeyer reaction. See: Clement, B.; Zimmerman, M. *Biochem. Pharmacol.* **1988**, 37, 4747. The present method affords the compound in higher yield.

Table VIII. Crystallographic Data

compd	4 (E = S)	4 (E = Se)	5 (E = S, α -phase)	5 (E = Se)	5 (E = S, β -phase)	6 (E = Se)
formula	$C_8H_4N_3S_2$	$C_8H_4N_3Se_2$	$C_8H_4N_3S_2$	$C_8H_4N_3Se_2$	$C_8H_4N_3S_2$	$C_8H_4N_3Se_2$
fw	206.3	300.06	206.3	300.06	206.3	300.06
<i>a</i> , Å	10.466 (3)	10.478 (4)	7.295 (3)	7.364 (8)	8.782 (1)	7.301 (1)
<i>b</i> , Å	10.342 (2)	10.780 (4)	20.488 (2)	21.085 (4)	5.638 (1)	11.883 (2)
<i>c</i> , Å	9.169 (2)	9.432 (4)	11.267 (2)	11.119 (4)	17.128 (4)	10.186 (1)
α , deg	104.97 (2)	107.16 (3)				
β , deg	112.97 (2)	115.23 (2)	95.54 (2)	94.91 (5)	102.94 (2)	101.50 (1)
γ , deg	69.84 (2)	68.39 (3)				
<i>V</i> , Å ³	849.0 (3)	883.8 (6)	1676.0 (7)	1720 (2)	826.5 (6)	866.1 (5)
<i>d</i> (calcd), g cm ⁻³	1.61	2.255	1.635	2.317	1.66	2.301
<i>Z</i>	4	4	8	8	4	4
λ , Å	0.71073	0.71073	0.71073	0.71073	0.71073	0.71073
space group	<i>P</i> $\bar{1}$	<i>P</i> $\bar{1}$	<i>P</i> $2_1/n$	<i>P</i> $2_1/n$	<i>P</i> $2_1/n$	<i>P</i> 2_1
<i>T</i> , K	293	293	293	293	293	293
μ , cm ⁻¹	5.5	82.3	5.6	84.6	5.6	84.0
<i>R</i> , <i>R</i> _w ^a	0.037, 0.057	0.049, 0.059	0.057, 0.070	0.079, 0.089	0.028, 0.036	0.050, 0.054

$$^a R = [\sum |F_o| - |F_c|] / [\sum |F_o|]; R_w = \{[\sum w|F_o| - |F_c|]^2 / [\sum w(F_o)^2]\}^{1/2}.$$

Et₂O. The N-lithio species was precipitated in virtually quantitative yield and was used without further purification in subsequent reactions.

Preparation of [4-NCC₆H₄(CN₂Se₂)]. 4-Cyanobenzamidine (5.07 g, 35 mmol) and SCl₂ (5 mL, excess) were stirred in 100 mL of hot acetonitrile for 1 h. The orange precipitate of crude dithiadiazolium chloride was filtered off, washed with acetonitrile, and dried in vacuo. The intermediate was then washed back to the reaction flask with 100 mL of acetonitrile, and triphenylantimony (6.30 g, 18 mmol) was added. The resulting dark slurry was stirred for 30 min at room temperature. The dark blue/black precipitate was filtered, washed with acetonitrile, dried in vacuo, and sublimed to give 1.25 g (17%) of blue/black crystals, 160–163 °C dec. IR (Nujol mull, 2000–250 cm⁻¹): 1463 (s), 1410 (m), 1376 (s), 1365 (s), 1313 (m), 1267 (m), 1198 (w), 1189 (w), 1171 (m), 1138 (s), 1105 (w), 1017 (w), 849 (s), 835 (s), 816 (s), 782 (s), 731 (m), 652 (s), 543 (s), 508 (s), 450 (m), 400 (m) cm⁻¹; ν (CN) 2228 cm⁻¹. Mass spectrum: *m/e* 206 (M⁺, 84%), 160 (M - NS)⁺, 34%, 128 (NCC₆H₄CN⁺, 41%), 78 (S₂N⁺, 100%), 64 (S₂⁺, 18%). Anal. Calcd for C₈H₄N₃Se₂: C, 46.59; H, 1.95; N, 20.37; S, 31.09. Found: C, 46.72; H, 2.18; N, 20.18; S, 30.88.

Preparation of [4-NCC₆H₄(CN₂Se₂)]. Solid N-lithio-N',N'-bis(trimethylsilyl)-4-cyanobenzamidine (3.02 g, 0.01 mol) was added to a solution of SeCl₂ (generated in situ by mixing SeCl₄ (2.34 g) and selenium powder (0.82 g), in 100 mL of acetonitrile). The mixture was heated to reflux for 90 min, cooled, and filtered to yield crude [4-NCC₆H₄(CN₂Se₂)]⁺Cl⁻ (contaminated with LiCl) as a dark red powder. This solid was slurried in 120 mL of acetonitrile, solid Ph₃Sb (1.89 g, 5.4 mmol) was added, and the mixture was refluxed for 20 min. The resulting black solid was filtered out, washed with 30 mL of CH₃CN, and dried in vacuo. Crude [4-NCC₆H₄(CN₂Se₂)] was sublimed at 130 °C/10⁻² Torr to give black crystals, 240–243 °C dec (yield 20%). IR (Nujol mull, 2000–200 cm⁻¹): 1495 (w), 1463 (s), 1407 (m), 1377 (s), 1317 (s), 1285 (m), 1197 (w), 1188 (w), 1169 (m), 1125 (s), 1104 (w), 1017 (w), 969 (w), 877 (w), 845 (s), 835 (s), 765 (m), 741 (m), 730 (w), 697 (w), 677 (s), 655 (m), 641 (m), 542 (s), 506 (w), 447 (s), 410 (s), 250 (m) cm⁻¹; ν (CN) 2227 cm⁻¹. Mass spectrum: *m/e* 302 (M⁺, 63%), 174 (Se₂N⁺, 100%), 128 (NCC₆H₄CN⁺, 26%). Anal. Calcd for C₈H₄N₃Se₂: C, 32.02; H, 1.34; N, 14.00. Found: C, 32.20; H, 1.20; N, 14.23.

Preparation of [3-NCC₆H₄(CN₂Se₂)]. This material was prepared in a manner identical to that described for the 4-cyano-substituted derivative; yields were similar. Sublimation at 120 °C/10⁻² Torr afforded pure [3-NCC₆H₄(CN₂Se₂)] as a mixture of deep red needles (α -phase) and blocks (β -phase). The two phases were separated manually. Total yield: 0.96 g (23%), α -phase 157–160 °C dec, β -phase 165–168 °C dec. IR (Nujol mull, 2000–200 cm⁻¹): α -phase 1464 (s), 1375 (s), 1291 (m), 1260 (m), 1196 (s), 1175 (w), 1117 (m), 1100 (w), 1092 (w), 1000 (w), 987 (w), 953 (m), 936 (w), 903 (m), 840 (s), 810 (s), 793 (m), 776 (s), 723 (w), 690 (s), 569 (m), 560 (m), 506 (s), 471 (w) cm⁻¹; ν (CN) 2230 cm⁻¹; β -phase 1462 (s), 1365 (s), 1288 (m), 1257 (m), 1200 (s), 1167 (m), 1131 (w), 1119 (m), 1089 (s), 997 (w) 955 (s), 916 (s), 850 (s), 798 (s), 787 (s), 722 (w), 689 (s), 666 (w), 567 (s), 511 (s), 473 (w), 439 (w), 388 (w), 259 (m) cm⁻¹; ν (CN) 2231 cm⁻¹. Mass spectrum: *m/e* 206 (M⁺, 70%), 160 (M - NS)⁺, 26%, 128 (NCC₆H₄CN⁺, 29%), 78 (S₂N⁺, 100%), 46 (SN⁺, 12%). Anal. Calcd for C₈H₄N₃Se₂: C, 46.59; H, 1.95; N, 20.37; S, 31.09. Found: C, 46.33; H, 2.11; N, 20.45; S, 31.03.

Preparation of [3-NCC₆H₄(CN₂Se₂)]. This material was prepared (with comparable yield) in a manner identical to that described for the 4-cyano-substituted derivative. The product was purified by repeated

vacuum sublimation at 130 °C/10⁻² Torr to produce green-black needles, 265–267 °C dec. IR (Nujol mull, 2000–200 cm⁻¹): 1463 (s), 1377 (s), 1321 (m), 1310 (m), 1302 (m), 1260 (w), 1192 (s), 1172 (w), 1110 (w), 1097 (w), 1020 (w), 983 (w), 933 (m), 928 (w), 901 (m), 806 (s), 791 (m), 773 (w), 741 (s), 723 (w), 702 (w), 692 (s), 618 (s), 569 (s), 559 (w), 472 (m), 405 (s), 289 (m), 279 (m) cm⁻¹; ν (CN) 2228 cm⁻¹. Mass spectrum: *m/e* 302 (M⁺, 58%), 174 (Se₂N⁺, 100%), 128 (NCC₆H₄CN⁺, 19%). Anal. Calcd for C₈H₄N₃Se₂: C, 32.02; H, 1.34; N, 14.00. Found: C, 32.11; H, 1.24; N, 13.84.

Preparation of [2-NCC₆H₄(CN₂Se₂)]. A solution of SeCl₂ was prepared in situ from a slurry of SeCl₄ (2.2 g, 10 mmol) and selenium powder (0.8 g, 10 mmol) in 100 mL of CH₃CN. Compound 7 (3.6 g, 10 mmol) was then added to the solution as a dry powder, and the mixture was heated for 2 h. The red-brick precipitate was removed by filtration and washed with 40 mL CH₃CN. This material (crude [2-NCC₆H₄(CN₂Se₂)]Cl) was then reduced by heating it with triphenylantimony (1.5 g, 5 mmol) in 100 mL of refluxing CH₃CN. The black solid so produced was filtered out and pumped dry in vacuo. Slow sublimation at 140 °C/0.1 Torr produced a mixture of lustrous coppery blocks (220–23 °C dec) and a few feathery needles (192–93 °C dec) of [2-NCC₆H₄(CN₂Se₂)]. The two phases were separated manually. IR of block phase (Nujol mull, 2000–200 cm⁻¹): 1441 (m), 1337 (m), 1300 (m), 1282 (m), 1142 (m), 1085 (m), 782 (w) 762 (m), 749 (s), 731 (s), 704 (s), 691 (s), 649 (s), 624 (w), 569 (m), 555 (s), 506 (m), 394 (w), 385 (m), 288 (m) cm⁻¹; ν (CN) 2224 cm⁻¹. Mass spectrum: *m/e* 302 (M⁺, 52%), 174 (Se₂N⁺, 100%), 128 (NCC₆H₄CN⁺, 25%). Anal. Calcd (of blocks) for C₈H₄N₃Se₂: C, 32.02; H, 1.34; N, 14.00. Found: C, 32.15; H, 1.13; N, 13.99.

X-ray Measurements. X-ray data were collected on either an Enraf-Nonius CAD-4 or a Rigaku AFC5R with monochromated Mo K α radiation; the latter employed a 12-kW rotating-anode generator. Data were collected using a $\theta/2\theta$ technique and the structures were all solved by direct methods and refined by full-matrix least squares which minimized $\sum w(\Delta F)^2$. No extinction corrections were made. A summary of crystallographic data is provided in Table VIII. Special points pertaining to individual structures are summarized below.

[4-NCC₆H₄(CN₂Se₂)]. The crystals have a strong tendency to twin. The crystal chosen for data collection was the least twinned of numerous crystals examined. Because of the anomalous backgrounds attributed to twin components, six reflections were given zero weight in the full-matrix least-squares refinement. The relatively high value of *R* and the large thermal ellipsoids with shapes and orientations which are marginally acceptable are also ascribed to unknown effects of this twinning on the data set collected. The largest peaks on the final difference map were located midway between the Se atoms along the lines of the dimerization linkages.

α -[3-NCC₆H₄(CN₂Se₂)]. Both of these compounds produce twinned crystals upon sublimation. The twinning was much more of a problem for the selenium derivative. Numerous crystals were mounted on the diffractometer; many were twinned so badly that the main lattice could not be found. In the selenium case the high merge for duplicate data and significant intensity for several symmetry-forbidden reflections also indicated a twin component. The data sets used for refinement represent the best we found, but both the refinements had to involve nonroutine procedures to overcome the effects of twinning on the data. In both cases this included giving zero weight to particular zones of reflections for which all had $F_o \gg F_c$. Only those reflections which had ΔF values significantly greater than the largest ΔF for reflections with $F_o < F_c$ were zero-weighted. For the sulfur crystal this involved 17 reflections, 16 of

which had $h = 3$. For the Se crystal 40 reflections were excluded using the above criteria, of these 32 had $h = 4$. In the Se crystal difference map peaks in the general plane of the Se atoms of the dimer indicated the possible nature of the major contributors to this twinning; there were peaks at Se–Se separations consistent with the displacements of the dimer unit along the Se–Se 3.2-Å vectors. Two sets of four Se positions (as if two more dimer units were interstitial with the main unit) were included in the refinement. These fractional Se atoms were constrained to map positions with isotropic B values set at 3, and the multiplicities were refined. One set (which had positions of approximately $x = 0.28$, y , z , of the main dimer) refined to an occupancy factor of 0.063. The other set (at $x = 0.16$, y , z) refined to an occupancy factor of 0.037. The inclusion of these traces of Se atoms led to a significant reduction of the highest difference map residual and, perhaps more significantly, produced a refinement with much more reasonable values for the isotropic thermal parameters of the N and C atoms. Inclusion of complete dimer units

attached to these Se positions and parallel to the main dimer unit gave some additional improvement, but in view of the fact that the parallelism was arbitrary, this model was not used. Only the Se positions indicated by difference maps were used as outlined above.

Acknowledgment. Financial support at Guelph was provided by the Natural Sciences and Engineering Research Council of Canada and at Arkansas by the National Science Foundation (EPSCOR program) and the State of Arkansas.

Supplementary Material Available: Tables of structure solution and refinement data (S1), hydrogen atom coordinates (S2), bond lengths and angles (S3 and S4), and anisotropic thermal parameters (S5–S8) for the six structures reported (12 pages); listings of observed and calculated structure factors (101 pages). Ordering information is given on any current masthead page.

Contribution from the Department of Chemistry,
Wayne State University, Detroit, Michigan 48202

Approaches to Hexane-Soluble Cationic Organometallic Lewis Acids. Synthesis, Structure, and Reactivity of Titanocene Derivatives Containing Polysilylated Cyclopentadienyl Ligands

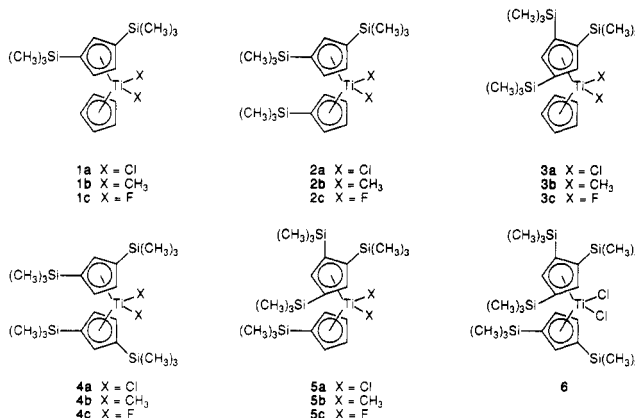
Charles H. Winter,* Xiao-Xing Zhou,¹ and Mary Jane Heeg

Received November 7, 1991

A series of titanocene dichloride derivatives was synthesized where the total trimethylsilyl substitution on the two cyclopentadienyl rings was 0, 2, 3, 4, and 5. Treatment of these complexes with methylolithium afforded 88–93% yields of the dimethyl derivatives, while reaction of the dichlorides with silver tetrafluoroborate afforded 45–57% yields of the difluoro derivatives. However, 1,1',2,3',4-pentakis(trimethylsilyl)titanocene dichloride afforded complex reaction mixtures upon treatment with either methylolithium or silver tetrafluoroborate. Complexes containing three and four trimethylsilyl groups afforded moderately stable cationic intermediates. The cationic complex derived from 1,1',3,3'-tetrakis(trimethylsilyl)titanocene dichloride and silver tetrafluoroborate was the most stable and was partially characterized by ¹H, ¹⁹F, and ¹³C NMR and IR spectroscopy. The barrier to cyclopentadienyl rotation was examined for 1,1',3,3'-tetrakis(trimethylsilyl)titanocene dichloride and 1,1',3,3'-tetrakis(trimethylsilyl)titanocene difluoride and was found to be 8.9 ± 0.5 kcal/mol for both complexes. The X-ray crystal structures of 1,1',3,3'-tetrakis(trimethylsilyl)titanocene difluoride and 1,1',2,4-tetrakis(trimethylsilyl)titanocene difluoride were determined to probe for steric distortions. 1,1',3,3'-Tetrakis(trimethylsilyl)titanocene difluoride crystallizes in the orthorhombic space group $Pbna$ with $a = 8.788$ (9) Å, $b = 18.093$ (2) Å, $c = 18.585$ (2) Å, $V = 2954.8$ (9) Å³, and $Z = 4$. 1,1',2,4-Tetrakis(trimethylsilyl)titanocene difluoride crystallizes in the triclinic space group $P\bar{1}$ with $a = 9.2476$ (5) Å, $b = 10.6838$ (15) Å, $c = 15.8842$ (19) Å, $\alpha = 106.754$ (10)°, $\beta = 96.727$ (8)°, $\gamma = 99.291$ (8)°, $V = 1456.9$ (3) Å³, and $Z = 2$.

Transition metal complexes bearing bulky substituted cyclopentadienyl ligands often exhibit properties very different from those of the corresponding unsubstituted cyclopentadienyl analogues.^{2,3} Although much of the chemistry of substituted cyclopentadienyl ligands has centered around the pentamethylcyclopentadienyl (Cp*) ligand,³ other bulky cyclopentadienyl ligands have been employed.^{4–10} Relatively little work has ap-

Chart I



peared concerning transition metal complexes containing silylated cyclopentadienyl ligands.^{5–9} Initial investigations have clearly

- (1) Wilfred Heller Fellow, 1991–1992.
- (2) Thomas, J. L.; Brintzinger, H. H. *J. Am. Chem. Soc.* **1972**, *94*, 1386. Thomas, J. L. *Ibid.* **1973**, *95*, 1838. King, R. B.; Efraty, A. *Ibid.* **1972**, *94*, 3773. King, R. B.; Efraty, A.; Douglas, W. M. *J. Organomet. Chem.* **1973**, *56*, 345.
- (3) For leading references, see: Maitlis, P. M. *Acc. Chem. Res.* **1978**, *11*, 301. Wolczanski, P. T.; Bercaw, J. E. *Ibid.* **1980**, *13*, 121. McLain, S. J.; Sancho, J.; Schrock, R. R. *J. Am. Chem. Soc.* **1979**, *101*, 5451. Manriquez, J. M.; Fagan, P. J.; Marks, T. J. *Ibid.* **1978**, *100*, 3939. Sikora, D. J.; Rausch, M. D.; Rogers, R. D.; Atwood, J. L. *Ibid.* **1981**, *103*, 1265. Freyberg, D. P.; Robbins, J. L.; Raymond, K. N.; Smart, J. C. *Ibid.* **1979**, *101*, 892. King, R. B. *Coord. Chem. Rev.* **1976**, *20*, 155. Schmid, G. F.; Brookhart, M. *J. Am. Chem. Soc.* **1985**, *107*, 3508. Jeske, G.; Lauke, H.; Mauermann, H.; Swepston, P. N.; Schumann, H.; Marks, T. J. *Ibid.* **1985**, *107*, 8091.
- (4) For leading references, see: Chambers, J. W.; Baskar, A. J.; Bott, S. G.; Atwood, J. L.; Rausch, M. D. *Organometallics* **1986**, *5*, 1635. Heeg, M. J.; Janiak, C.; Zuckerman, J. J. *J. Am. Chem. Soc.* **1984**, *106*, 4259. See also: Lorbeth, J.; Shin, S.-H.; Wocadlo, S.; Massa, W. *Angew. Chem., Int. Ed. Engl.* **1989**, *28*, 735.

- (5) For example, see: Jutzi, P.; Schlüter, E.; Krüger, C.; Pohl, S. *Angew. Chem., Int. Ed. Engl.* **1983**, *22*, 994. Morley, C. P.; Jutzi, P.; Krüger, C.; Wallis, J. M. *Organometallics* **1987**, *6*, 1084.